An EXAFS study of the nanocrystalline transformation of ZrO_2:Y_2O_3(5%)

2001 J. Phys.: Condens. Matter 13 11503

(http://iopscience.iop.org/0953-8984/13/50/309)

INSTITUTE OF PHYSICS PUBLISHING JOURNAL OF PHYSICS: CONDENSED MATTER

J. Phys.: Condens. Matter **13** (2001) 11503–11509 PII: S0953-8984(01)27056-8

An EXAFS study of the nanocrystalline transformation of ZrO_2:Y_2O_3(5%)

Zeming Qi[1,6], Chaoshu Shi[1,2], Yaguang Wei[1], Zheng Wang[2], Tao Liu[3], Tiandou Hu[3], Zongyan Zhao[4] and Fuli Li[5]

[1] National Synchrotron Radiation Laboratory, University of Science and Technology of China, Hefei, Anhui 230029, People's Republic of China
[2] Department of Physics, University of Science and Technology of China, Hefei, Anhui 230026, People's Republic of China
[3] Institute of High Energy Physics, Chinese Academy of Sciences, Beijing 100039, People's Republic of China
[4] Department of Physics, Anhui University, Hefei, Anhui 230039, People's Republic of China
[5] Department of Physics, Capital Normal University, Beijing 100037, People's Republic of China

E-mail: zmqi@ustc.edu.cn

Received 1 April 2001, in final form 14 September 2001
Published 30 November 2001
Online at stacks.iop.org/JPhysCM/13/11503

Abstract

Nanostructured zirconia doped with 5% yttria was prepared by a co-precipitate method. The structures were characterized by x-ray diffraction and extended x-ray absorption fine structure spectroscopy. The sample calcined at 300°C had an amorphous phase and a local structure like cubic zirconia. It crystallized into tetragonal nanocrystalline zirconia at 500 °C and the monoclinic phase appeared at 900 °C. The Y atoms merged into the zirconia network at 300 °C, with the oxygen vacancies located around the Zr atoms. The coordination number of the cation-cation reduction is due to the large amount of cations near the surface with fewer nearest neighbours when the grain size decreases.

1. Introduction

Zirconia (ZrO_2) is an important ceramic material with useful mechanical, thermal, optical and electrical properties [1–3]. These outstanding properties have been put to use in many applications such as catalysis, sensors, solid-state fuel cells and so on. Not only are the mechanical and electrical properties remarkable, zirconia is also interesting as a structural material. It can form cubic, tetragonal and monoclinic or orthorhombic phases at high pressure. At room temperature, only the monoclinic form is stable. Nevertheless, tetragonal and cubic phases can be formed at room temperature by adding oxides of metals to zirconia in appropriate proportions. The structural, mechanical and electrical properties of crystalline

[6] Corresponding author.

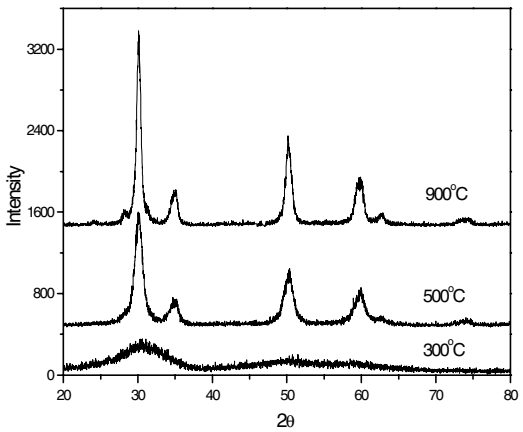

Figure 1. XRD pattern of ZrO_2/Y_2O_3 (5%) for different heat treatment temperatures.

zirconia have been extensively studied, but recently nanocrystalline zirconia has also attracted attention because the material properties are drastically altered by the reduction of grain size. For example, nanostructured zirconia has low thermal conductivity, reduced sintering temperature and improved mechanical properties. In order to understand the basic features of nanostructured zirconia it is necessary to obtain information on its atomic structure during its process of formation.

Extended x-ray absorption fine structure spectroscopy (EXAFS) is a powerful probe for local structure characterization. It is widely used for studying the short-range order in crystalline, amorphous and other disordered systems. Li *et al* have published a complete work on the ZrO_2/Y_2O_3 system [4–6]. However, their studies focused on crystalline zirconia. In the present work, yttria-stabilized (5%) nanocrystalline zirconia was obtained by a co-precipitate method. The crystallization from the amorphous into the nanocrystalline state was characterized using x-ray diffraction. The local structures of the nanocrystallite were determined by EXAFS spectroscopy.

2. Experiment

2.1. Sample preparation

The ZrO_2/Y_2O_3 samples were prepared by the co-precipitate method. First, zirconyl chloride ($ZrOCl_2{\cdot}8H_2O$) was dissolved in water. Next, an adequate amount of YCl_3 was dissolved into the solution to give 5% yttria doped zirconia, then NaOH was added to this mixture until the pH = 13. The reaction product was filtered and washed by deionized water repeatedly, then dried at 80 °C for 48 hours. In order to obtain nanostructured ZrO_2/Y_2O_3 powders of different grain sizes, three groups of the precipitates underwent thermal treatment at 300 °C, 500 °C and 900 °C in air, respectively.

2.2. X-ray diffraction

X-ray diffraction (XRD) measurement was carried out by an MAC Science 18AHF diffractometer with CuK_α radiation. The intensity was measured in the 2θ range between 20 ° and 80 ° with a 2θ step of 0.02 °.

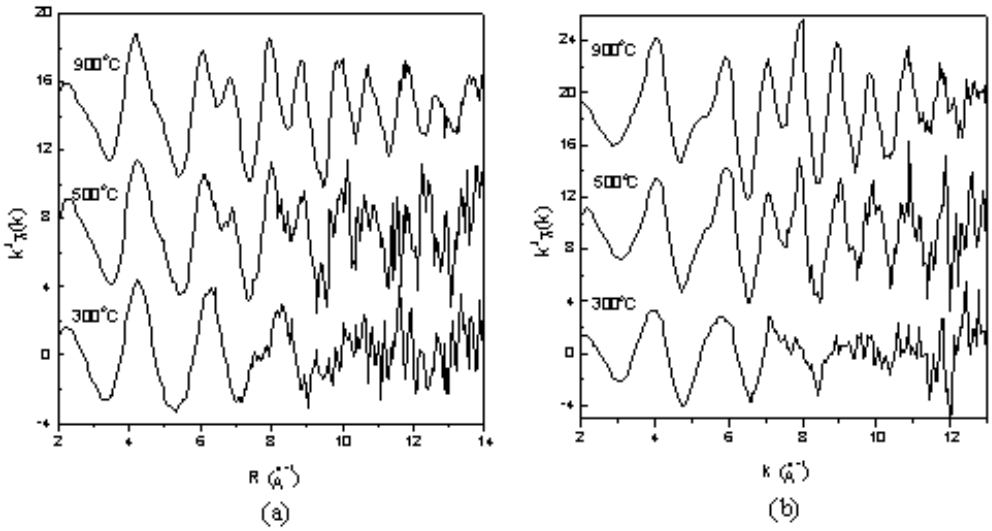

Figure 2. EXAFS of the Zr K-edge (a) and Y K-edge (b).

2.3. EXAFS measurement

X-ray absorption measurements at the Zr K-edge and Y K-edge were made on beamline 4W1B at the Beijing Synchrotron Radiation Laboratory. Energy selection was accomplished by using a double-crystal monochromator with a Si(111) crystal. All spectra were measured at room temperature in the transmission mode.

3. Data analysis and results

3.1. X-ray diffraction

The x-ray diffraction patterns of different thermal treatment samples are shown in figure 1. Up to 300 °C only an amorphous phase is present. With increasing treatment temperature, the grain size becomes larger and the phase becomes more ordered. Diffraction patterns of samples calcined at 500 °C and 900 °C have broad peaks that could be associated with either a tetragonal or a cubic phase. The observable difference between the cubic and tetragonal phases was the presence of the (012) reflection in the tetragonal phase, and the splitting of the (002), (113) and (004) reflections of the cubic phase into two peaks of the tetragonal phase (002), (110), (013), (121) and (004), (220), respectively. In the present case, we cannot be certain that it is a tetragonal phase because of broad diffraction peaks due to the small crystallite size. However, our EXAFS analysis confirm that the phase is indeed tetragonal. We also note that a monoclinic phase appears in the sample calcined at 900 °C but not in the 500 °C one. From the Scherrer equation, the crystallite sizes of the samples calcined at 500 °C and 900 °C are 9 nm and 15 nm, respectively.

3.2. EXAFS

The EXAFS data were analysed by the UWXAFS software package [7] The EXAFS signal $\chi(k)$ is defined as the normalized oscillatory part of the x-ray absorption coefficient and is

given by

$$\chi(k) = \frac{\mu(k) - \mu_0(k)}{\Delta\mu_0} \tag{1}$$

where $\mu(k)$ is the measured x-ray absorption coefficient and $\mu_0(k)$ is the smooth atomic background; k is the photoelectron wave number given by $k = \sqrt{2m(E - E_0)/\hbar^2}$ and E_0 is the energy threshold; $\Delta\mu_0$ is the absorption edge jump.

For disordered systems, the standard EXAFS formula can lead to non-negliglible errors in structural parameters when only a small Gaussian disorder is considered and the distribution of interatomic distances is completely characterized by its mean value and width. Therefore, amplitude and phase corrections in the EXAFS formula must be made. The cumulant expansion method [8] provides a model-independent approach to characterizing the shape of the distribution. Up to the fourth cumulant, the EXAFS equation can be written as:

$$\chi(k) = \sum_j \frac{N_j S_0^2(k) F_j(k)}{kR_j^2} \exp(-2k^2\sigma^2 + \frac{2}{3}C_4k^4) \exp(-2R_j/\lambda) \sin[2kR_j + \phi_j(k) - \frac{4}{3}C_3k^3] \tag{2}$$

where S_0^2 is the amplitude reduction factor, N_j the coordination number of the ith shell, R_j the bond length, σ_j the mean-square relative displacement, and C_{3j} and C_{4j} are the third and fourth cumulant, respectively; $F_j(k)$ and $\delta_j(k)$ are the effective scattering amplitude and phase shift, respectively, and $\lambda(k)$ is the mean free path of the photoelectron.

EXAFS analysis was performed at both the Zr and the Y K-edges. The pre-edge and post-edge of the raw EXAFS spectra were subtracted. The extraction of the EXAFS signal $\chi(k)$ was weighted by k^3 and is shown in figure 2. It is clear that the $\chi(k)$ of the sample calcined at 300 °C has a simpler local structure, which is consistent with an amorphous structure. The EXAFS spectra for the Zr and Y K-edges are obviously different in their shape, amplitude and frequency, implying different local structure. The Fourier transforms are shown in figure 3. Both Zr and Y K-edges reveal only two distinct peaks. The first peaks correspond to the Zr–O and Y–O coordination shells, respectively. The second peaks correspond to the cation-cation coordination shell. The Y–O peak has no obvious change when the calcination temperature increases, while the Zr–O peak is slightly lower. However, the heights of the second peaks increase rapidly with increasing temperature. A better appreciation of the difference in each shell for different calcination temperatures can be obtained by isolating each shell contribution through Fourier filtering. These data were back transformed to k space and are shown in figure 4. The coordination number CN, bond length R, Debye–Waller factor and the third cumulant C_3 were used as fitting parameters in the curve-fitting procedure. The scattering amplitudes and phase-shift functions were calculated using the FEFF code [9] The amplitude reduction factors S_0^2 of Zr and Y were obtained by fitting the data of bulk ZrO_2 and Y_2O_3, which gave 0.92 for the Zr K-edge and 0.9 for the Y K-edge. The results after quantitative fitting are summarized in table 1.

4. Discussion

4.1. Cation–O shell

The fitting results show that the Zr–O shell bond lengths at different calcination temperatures are longer than those of the bulk sample (2.13 Å) [5]. The Zr–O shell coordination numbers of samples at lower calcination temperatures are smaller than those of bulk samples. The bond length contracts and the coordination number decreases with increasing calcination

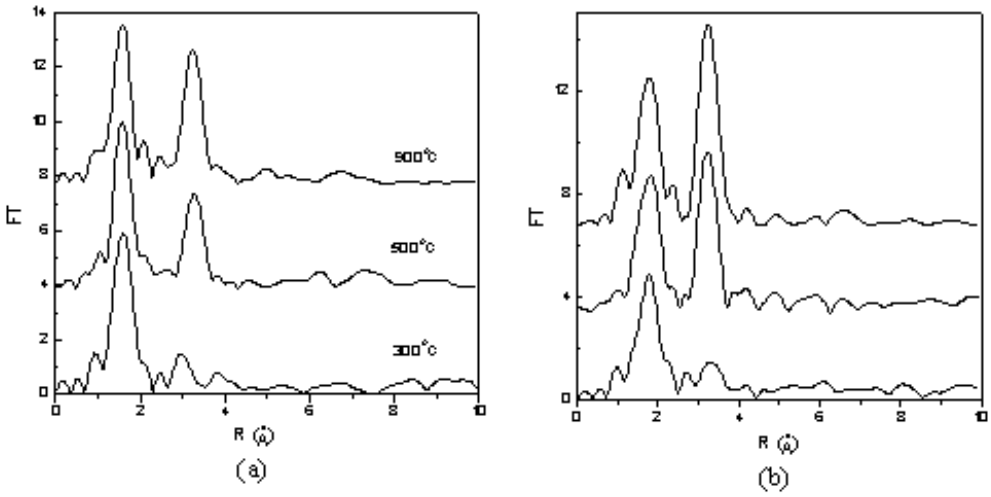

Figure 3. Fourier transform of Zr K-edge (a) and Y K-edge (b)

Table 1. EXAFS results of zirconia doped with 5% ytria

Edge	Sample (°C)	CN Cation-O	R (Å)	σ^2 (10^{-3})	C_3 (10^{-3})	CN Cation–cation	R (Å)	σ^2 (10^{-3})	C_3 (10^{-3})
Zr	900	4.1(4)	2.20(2)	4.9(10)	1.118(2)	7.5(10)	3.64(2)	9.3(6)	0.111(3)
	500	4.2(5)	2.21(2)	5.3(10)	1.451(2)	6.9(10)	3.63(2)	12.0(10)	0.103(3)
	300	5.7(5)	2.26(2)	8.6(8)	1.894(4)	4.9(10)	3.46(3)	16.1(30)	0.312(4)
Y	900	8.0(5)	2.33(1)	8.6(5)	0.136(2)	12(15)	3.64(2)	8.9(3)	0.043(3)
	500	8.0(5)	2.38(2)	11.0(10)	0.846(9)	8.7(10)	3.62(2)	9.0(5)	0.205(4)
	300	7.4(6)	2.43(2)	11.7(12)	1.608(5)	5.5(10)	3.60(2)	15.6(30)	0.963(13)

temperature. According to the results of Li *et al* [4–6], only one subshell of the Zr–O shell in the tetragonal phase can be seen at room temperature, while the other subshell contributes only to a broad background. Therefore, the low coordination number (fourfold coordination) and short bond length obtained should not be interpreted as the loss of oxygen atoms, but should be attributed to the fact that samples calcined above 500 °C are in the tetragonal phase. This is in agreement with the x-ray diffraction results of Bokhimi *et al* [10]. For the sample calcined below 300 °C, we think that it is in a local cubic phase structure. This transformation was also observed by Yuren Wang *et al* when studying pure nanocrystalline zirconia [11]. However, this result is different from our study of ZrO_2 doped with 15%Y_2O_3, which has a cubic phase when calcined above 500 °C [12]. Therefore, different Y_2O_3 concentrations can give rise to different phases during crystallization.

All the Y–O shells have the same coordination number (eightfold coordination), which indicates that the Y atoms have merged with the zirconia network after 300 °C heat treatment. Comparing the O-coordination around Zr atoms with that around Y atoms, we can conclude that the oxygen vacancies induced by doping Y atoms are located near the Zr atoms. The Y–O bond lengths of samples calcined at 300 °C are longer than those in Y_2O_3, due to the amorphous character. When the calcination temperature is increased, the Y–O bond length contracts more than the Zr–O bond length, as in the case of the bulk sample at 900 °C. This means that the local structure of the Y atom becomes closer to that of the bulk sample with increasing

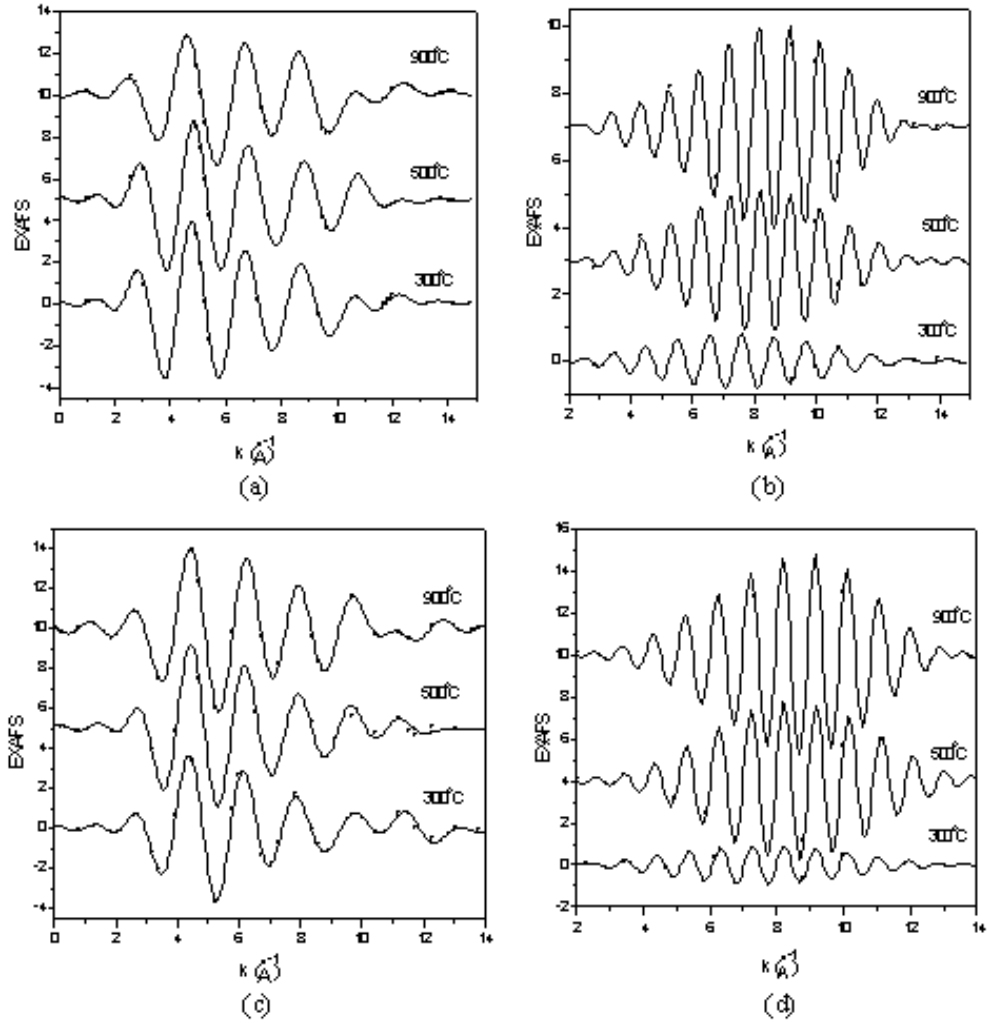

Figure 4. EXAFS of Zr-O shell (a), Zr-cation shell (b), Y-O shell (c) and Y-cation shell (d). Dotted line: experiment; solid line: fitted curve.

calcination temperature. The Debye–Waller factor and C_3 decrease with increasing calcination temperature, indicating that the sample becomes more ordered as a result of crystallization.

4.2. Cation–cation shell

The fitting results show that the Y–cation shell of the sample calcined at 900 °C has a similar coordination number to that of the bulk sample, while the Zr–cation shell appears to have a smaller one. Both Zr–cation and Y–cation shell coordination numbers decrease with decreasing particle size, the Y–cation number decreasing faster than that of the Zr–cation. The obvious decrease of the cation–cation coordination can be explained by the fact that an increasing fraction of cations are located near the nanoparticle surface as the particle size decreases. Compared with Y atoms, Zr atoms prefer to congregate at the surface of a nanoparticle. With increasing calcination temperature, the fitting results show that the bond lengths become

longer and approach closer to the values of the tetragonal phase. As with the cation-O shell, the Debye–Waller factor $\mu\sigma^2$ and C_3 decrease with increasing calcination temperature, due to crystallization.

5. Conclusion

Samples of 5% yttria doped zirconia have been prepared by the co-precipitate method. The crystallization and local structure around Zr and Y atoms were studied by EXAFS using synchrotron radiation. The XRD results indicate that the sample calcined at 300 °C has an amorphous phase. As the calcination temperature is increased the sample crystallizes and the monoclinic phase appears at 900 °C. Our EXAFS results indicate that the amorphous phase has a local structure like the cubic phase. This transforms to the tetragonal phase when the calcination temperature is increased up to 500 °C. The Y atoms merge into the zirconia network at 300 °C. The reduction of the cation–cation coordination is due to the large amount of cations near the surface with fewer nearest neighbours.

6. Acknowledgements

This work is being supported by the National Natural Science Foundation of China under Grant No.19974025. We are grateful to the staff of Beijing Synchrotron Radiation Facility.

References

[1] Ryshkemitz E and Richardson D W 1985 *Oxide Ceramics: Phys. Chem. and Technol.* (New York: Academic)
[2] Meriani S (ed) 1989 *Zirconia'88: Adv. in Zirconia Sci. and Technol.* (New York: Elsevier)
[3] Lu G, Niura N and Yanazoe J 1997 *J. Mater. Chem.* **7** 1445
[4] Li P, Chen I W and Hahn J E P 1993 *Phys. Rev.* B **48** 10063
[5] Li p, Chen I W and Hahn J E P 1993 *Phys. Rev.* B **48** 10074
[6] Li P, Chen I W and Hahn J E P 1993 *Phys. Rev.* B **48** 10082
[7] Stern E A, Newville M, Ravel B and Yacoby Y 1995 *Physica* B 208–209 117
[8] Koningsberger D C and Prins R (ed) 1988 *X-ray Absorption: Principle, Application, Techniques of XAFS, SEXAFS and XANES.* (New York: John Wiley and Sons)
[9] Zabinsky S I *et al* 1995 *Phys. Rev.* B **52** 2995
[10] Bokhimi X *et al* 1999 *J. Solid State Chem.* **142** 409
[11] Wang Y R *et al* 1994 *J. Phys: Condens. Matter* **6** 633
[12] Qi Z M *et al* 2001 *Acta Physica Sinica* **50** 1318 (in Chinese)